A method for implementing the CSO surface correction hardware: Memo No. 1

Date: 18-Oct-2002. By the CSO staff.

1 Introduction

The Leighton Telescope of the Caltech Submillimeter Observatory has a parabolic antenna with a 10.4 meter aperture. Holographic measurements indicate that the antenna surface deviation from a perfect, best-fit parabola is less than 22 μm rms over a large range of zenith angles (ZA): $10° < ZA < 75°$ [1]. Although the surface figure error is low, receiver coupling efficiency at the 806 GHz ($\lambda = 372\mu$m) operating frequency is currently only 33%. According to a simplified form of the Ruze formula[2], the antenna gain should vary as $exp((-4\pi\epsilon/\lambda)^2)$ where is ϵ is the rms surface deviation and λ is receiver wavelength. This simplification of the Ruze formula gives a gain of about 60% indicating that there are errors not measured by the relatively low spatial resolution holography maps and/or assumptions required in the application of the simplified formula (e.g. relatively small figure errors, small correlated areas on the surface, etc.) are not met. Nevertheless, it is clear from the simplified Ruze formula that at the shortest receiver wavelengths, the quality of the surface figure,ϵ, is k ey. To obtain the best performance of the Leighton Telescope at the highest operating frequencies, an active surface control system is indicated.

The Leighton antenna surface is comprised of 84 hexagonal panels tied together at each corner and supported underneath by standoff rods at 99 places. Each of the 99 surface support points is stood off from the space frame backup structure by a 12.5 mm (1/2") diameter steel rod on a compound adjustment screw. The standoff rods vary from 18cm (7") (Ref. [3] says 15cm) long at the node points in the center of the antenna to 10 cm (4") at the edge. The purpose of these long support rods is to provide lateral flexibility "to avoid distortions due to different thermal expansions" of the surface aluminum panels and the steel backup structure[4, 3]. To further increase lateral flexibility, the panel ends of the round standoff rods have two orthogonal, flat sections machined into them: e.g., see Figure 7 in Ref. [4]).

The surface can be considered as a continuous meniscus mirror supported from 99 node points on the backup structure by the standoff rods[3]. To correct small residual errors left in the overall surface figure from imperfect panel setting and from the unavoidable gravitational deviations, it has long been realized that the length of the standoff rods under the "low" sections of the surface could be expanded by heating to match the high points. More recently it was realized that the rods could be not only heated, but also cooled if each support rod's temperature was individually controlled by a Peltier thermo-electric cooler (TEC). The main advantage of using a TEC is that since some rods are heated, and some cooled, the net heat dumped into the structure and surface panels is close to zero and the needed rod expansions (or contractions) are minimized. With the previously conceived heating only scheme, all the standoff rods would have to be heated to match the deviation in highest one.

With the newly implemented surface control system each of the 99 standoff rods can now be considered as an adjustable piston, pushing or pulling on the meniscus surface to deform it to the correct shape. As noted, the deviation from the best paraboloid is small, so the needed rod excursions are not large. The current system can heat or cool the rods $\pm 20^\circ$C from the ambient temperature which, translates into approximately $\pm 50\mu$m of change in rod length for the 18 cm rods.

The purpose of this memo is to describe a method for implementing this new capability.

2 Control system hardware

For the purposes of this memo, the concept of the control system hardware can be simplified to three main elements as indicated in Figure 1: node k; the hardware control channel; and, the control computer. Referring to the figure, node k has a TEC thermally contacted to its standoff rod. The temperature of the standoff rod is monitored by a thermistor with resistance $R_k(T)$, where T is the rod absolute temperature. $R_k(T)$ is converted to a voltage by current I_k and buffered by an amplifier in the "Hardware control channel for node k", see the figure. In the hardware controller, the voltage feedback from the thermistor, Vr_k is used to servo a power amplifier for the TEC. The amount of heat the TEC pumps from it's liquid cooled heatsink into the standoff rod is controlled by the drive current from its power amplifier. However, TEC's are more efficient at heating than cooling because of ohmic losses in the device (e.g., see http://www.melcor.com/formula.htm).

The set point for the servo is provided by voltage Vc_k which is generated by a computer algorithm in the control computer. The nature of the required computer algorithm is the subject of the rest of this memo.

3 Equations needed for implementing a control algorithm

The equations and algorithm needed for controlling the surface are represented schematically in Figure 1.

3.1 Representing surface deviations

From gravitational deformations of the telescope structure, the surface error at each node point is expected to have sinusoidal deviation dependent on zenith angle[5, 6, 1]. The expected form of the deviation at node point k, D_k, is given by the equation

$$D_k(ZA) = A_k Cos(ZA + \phi_k) + Q_k \tag{1}$$

where k is the node number (of the set of 99 nodes); D_k is deviation of the surface at node k from the best fit paraboloid (D_k is in the direction parallel to the optical axis); ZA is the zenith angle, A_k is an amplitude coefficient particular to node k; ϕ_k is a "phase" term, particular to node k; and, Q_k is physically established by changing rod standoff length by adjusting its length[1]. That is, the coefficients A_k and ϕ_k are expected to be constants of the telescope structure, but Q_k can be manipulated by adjusting the compound screw on the end of the standoff rod at node k. If active adjustment is not available, the set of Q_k's should be "tuned" to give the optimum surface over the range of ZA's the antenna will be used (*ibid.*). Even with an active adjustment scheme such as we have implemented, such surface tuning is still desirable so as to require the minimum active control inputs (*ibid.*).

In principle, the coefficients A_k and ϕ_k can be determined from computer modelling of the backup structure. The Q_k's can only be determined by direct measurement. For our purposes, all three coefficients are determined from surface maps made with the CSO holography system [7] over a range of observing angles.

3.2 The standoff rod set point temperature

Once the deviations of the surface from the best fit paraboloid are established by fitting Eq. 1 to the holography data, a scheme can be implemented for correcting the surface. However, besides accurate measurements of the surface, several other accurate calibrations must be achieved. The individual temperature expansion coefficient for each rod, G_k, must be reliably established; and the temperature/resistance calibration curve for the thermistor at each rod, $R_k(T)$, must be accurately measured; and, the current across each thermistor, I_k, must be a suitable value, and unchanging for all time and under all environmental conditions.

Once the G_k's are known, the required panel displacement at each node point can be used to calculate required temperature change, $\triangle T_k(ZA)$, required to adjust the surface to zero error:

$$\triangle T_k(ZA) = -G_k \times D_k(ZA) \tag{2}$$

The $\triangle T_k(ZA)$ may then be used to calculate the rod set point temperature Tc_k. It is well known that in order for the Leighton antenna to perform well the backup structure must be in thermal equilibrium with its surroundings. During a typical day, inside the CSO dome a large thermal gradient forms between the higher and lower levels of the building due to solar heating. After opening the dome in the evening it is commonly observed that about one hour of time is required for changing thermal gradients across the antenna to disappear. During this equilibration time, the changing thermal gradients are manifested by unstable antenna pointing characteristics. It is assumed that when the antenna stabilizes, the backup structure is of uniform temperature and equal to the ambient air temperature, T_{amb} [3](p. 69). During the night T_{amb} may change, but for reliable measurements it must change slowly enough that the antenna structure stays in equilibrium. Since the backup structure and the feed legs are all made of steel, an overall change in the shape of the support structure is not expected. All of the holography maps used to obtain the D_k's in Eq. (1) are obtained under these circumstances.

In order not to lock in an offset, or an early evening thermal gradient, the set of Tc_k's must track the temperature of the backup structure. Therefore we recommend using

$$Tc_k(ZA, Tamb) = \triangle T_k(ZA) + T_{amb} \tag{3}$$

to determine the rod set point temperature at node k. In Equation 3, Tc_k is shown as an explicit function of ZA and T_{amb}.

$Tc_k(ZA)$, must then be translated into the corresponding thermistor resistance, $Rc_k(ZA, Tamb)$. That can be done with the use of the Stienhart-Hart, Equation 5, which is described below.

3.3 The thermistor response

The temperature transducers being used in the system are from Fenwal Electronics and are nominally 10KΩ at 25° C. Fenwal Electronics Thermicalc calibration curve No. 12 applies. These thermistors have a nominal calibration curve represented by the solid line in the sub-block labeled "Temperature/Resistance calibration curve" in Figure 1. The actual devices are manufactured to a 20% tolerance, so the range of possible curves is represented by the dotted lines.

During night time the CSO operating temperature is typically near 0° C, but temperatures as low as −16° C have been recorded. Typical G_k's for the 18 cm standoff rods are approximately 2.5μm/°C. If a ±50μm excursion is required, then for typical conditions the range of control temperatures needed is ±20°C. The corresponding resistance range from inspecting Figure 1 is $100K\Omega > R > 10K\Omega$.

The thermistor temperature/resistance response is obviously non-linear but their performance can well characterized by the empirical Steinhart-Hart equations:

$$1/T = a_k + b_k ln(R) + c_k(ln(R))^3 \tag{4}$$

or

$$R = exp[(\frac{-\chi}{2} + (\frac{\chi^2}{4} + \frac{\psi^3}{27})^{1/2})^{1/3} + (\frac{-\chi}{2} - (\frac{\chi^2}{4} + \frac{\psi^3}{27})^{1/2})^{1/3}] \tag{5}$$

with

$$\chi = \frac{a_k - 1/T}{c_k}$$

and

$$\psi = b_k/c_k.$$

T is in degrees Kelvin, R is resistance in ohms. The three coefficients a_k, b_k, c_k are found by fitting Eq. 4 to actual measurements of the thermistor[8, 9]. For the Fenwal thermistors we are using, fitting the nominal resistance curve to Equation 4 gives ($a_k, b_k, c_k : 9.8019E-4, 2.4717E-4, 1.2449E-7$). It can be verified that when put back into Equation 5, this set of a_k, b_k, c_k matches the nominal Fenwal resistance curve to within 0.04%. Eq. 5 is valid if

$$\frac{\chi^2}{4} + \frac{\psi^3}{27} > 0. \quad (6)$$

Otherwise, the real roots of Eq. 4 are multiple valued. In that case, a non-unique analytical solution exists and can be used if care is taken to pick the right value, or Eq. 4 can be solved for R as a function of T in the expected range by a simple root finding method such as an iterative bisection routine.

In practice, it appears the condition in Eq. 6 is usually satisfied and Eq. 5 can be used.

3.4 Output to controller

With the $Rc_k(ZA, Tamb)$ determined, the control voltage, Vc_k, corresponding to temperature set point, Tc_k, can be determined from

$$Vc_k = Rc_k \times I_k \quad (7)$$

where I_k is the current across the thermistor.

4 Utility of the monitoring function

The hardware controller is equipped with the ability to read voltage output corresponding to the thermistor resistance and present the information back to the control computer: see Figure 1. This monitoring function can be implemented in a way which is useful for calibration and for automatically verifying instrument function once the surface control system is put into routine operation.

4.1 The monitoring function and calibration

The following method describes one possible system calibration scheme:

1. A well calibrated temperature probe can be thermally contacted with the standoff-rod/TEC assembly at node k. (A plunger, mechanical

dial indicator can also be mounted at this time to verify panel displacement).

2. The voltage corresponding to the thermistor resistance, Vr_k, can be read into the computer by the monitoring function. The operator performing the calibration should note both the temperature and the corresponding Vr_k.

3. The operator uses a computer program to force a new set point voltage, Vc_k, from the computer. When the set point voltage is obtained, as verified by the monitor function, the temperature probe (and panel displacement) are recorded.

4.2 The monitoring function and routine system operation

The feedback provided by the monitoring function will be very important for routine operations. The surface control program should be designed to use the monitoring function to continually read back the Vr_k's and verify that they converge to the correct values in a reasonable amount of time. If not, there may be a fault due to failed hardware or cabling. Some types of cabling failures may lead to run-away heating at the faulty node due to an open-loop condition in the servo. This type of situation should be avoided as we do not know if excessive heating of the epoxy bonding in the surface panels can cause long term damage such as dimensional creep or delamination.

Other reasons for automatically monitoring and detecting non-convergence in any of the Vr_k's include immediately alerting the technical staff to a problem condition, and alerting the telescope operator that the surface control system is malfunctioning and to shut it off. Ultimately, it will be best if the system is set up to shut itself off in the event of a detected hardware failure to avoid: (1) causing distortions in the surface; (2) and, to avoid any chance of long term damage due to excessive heating.

5 Conclusion

This memo tries to create a method that will give the correct commands to the surface control system under night time conditions when the sky is good and the when antenna is in equilibrium with the air temperature. It draws on our current knowledge from working with this system and from the literature. Some parts of the procedures outlined here are already implemented, and after additional experience is acquired, refinements in the above outlined procedures may be required. Therefore, this memo should be considered a working document subject to revision if indicated. Accordingly, it is numbered "Memo No. 1" with the expectation that more will follow.

References

[1] D. Woody, E. Serabyn, and A. Schinckel. Measurement, modeling and adjustment of the 10.4 m diameter leighton telescopes. In T. G. Phillips, editor, *Advanced Technology MMW, Radio, and Terahertz Telescopes*, volume 3357 of *SPIE Proceedings Series*, pages 474–485, Bellingham, WA 98227-0010, 1998. SPIE-The International Society for Optical Engineering.

[2] J. Ruze. Antenna tolerance theory - a review. *Proc. of the IEEE*, 54(4):633–640, 1996.

[3] D. Woody, D. Vail, and W. Schaal. Design, construction, and performance of the leighton 10.4-m-diameter radio telescopes. *Proc. of the IEEE*, 82(5):673–686, 1994.

[4] R. Leighton. A 10-meter telescope for millimeter and sub-millimeter astronomy. Final technical report for nsf grant 73-04908, California Institute of Technology, May 1978.

[5] S. von Hoerner and W. Y. Wong. Gravitional deformation and astigmatism of tiltable radio telescopes. *IEEE Trans. Ant. and Prop.*, AP-23:689–695, 1975.

[6] D. Woody. Gravitational deflection of the leighton telescope. In G. D. Watt and A. S. Webster, editors, *Submillimetre Astronomy*, pages 43–44. Kluwer Academic Publishers, 1990.

[7] E. Serabyn, T. G. Phillips, and C. R. Masson. Surface figure measurements of radio telescopes with a shearing interferometer. *Applied Optics*, 30(10):1227–1241, 1991.

[8] J. S. Steinhart and S. R. Hart. *Deep-Sea Res.*, 15:497, 1968.

[9] H. W. Trolander, D. A. Case, and R. W. Harruff. Reproducibility, stability and linearization of thermister resistance thermometers. In *Fifth Symposium on Temperature, Washington, D. C.*, pages 997–1009. Instrument Society of America, 400 Stanwix Street, Pittsburgh, PA 15222, June 1971.

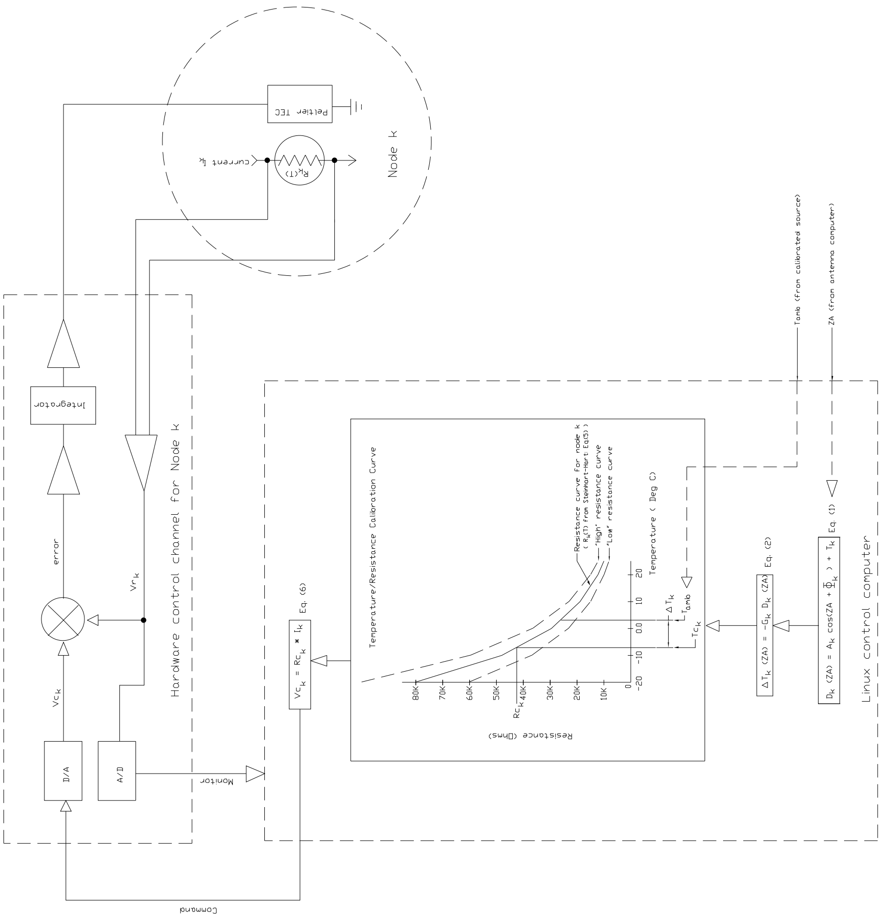

Figure 1: Block Diagram.